CHAPTER II

LITERATURE REVIEW

This chapter summarizes findings from previous research studies to enhance an understanding of the relationship between slake durability tests, erosional process, and related energy. The following contents are an overview of related topics, including (1) rock erosion process, (2) simulation of erosion and slake durability test, (3) erosional factors, and (4) erosive energy.

2.1 Rock erosion process

Erosion is one of the processes that governing the degradation behavior of rock. This process occurs through various mechanisms. It requires dynamic force within rock itself to cause the detachment (physical weathering) and the external forces to transport in an environment systems (Krautblatter & Moore, 2014; Paripuri, Parian, & Rosenkranz, 2020). Foye (1921) delineates two different mechanisms in the process: (1) mechanical erosion (corrasion) and (2) chemical erosion (corrosion). These mechanisms work in a similar way in the weathering process. Only the mechanical erosion requires motion of atmospheric action, and chemical erosion occurs to alter the internal components within rocks though action of chemical agents that present in the transporting environments.

2.2 Simulation of erosion and slake durability test

For simulating erosion, the laboratory and numerical models are extensively used by researchers to understand the impact of degradation process under severe conditions. Variety of techniques are employed to replicate the complex behaviors under wind and water, with the isolated and controllable of specific conditions through

simulation, it tend to provide specific factors that governing degradation corresponds to variation of rock types. Some of them are simulated by setting the external forces, including plunge pool, water and aerial jets (George & Sitar, 2012; Scheingross & Lamb, 2017; Xiang, Latham, & Pain, 2022). Figure 2.1 shows the schematic of plunge pool technique.

According to the state reviews of Moses, Robinson, and Barlow (2014). Several researchers are precisely calibrated the laboratory and numerical simulation results against field data to reflect each rock in the environmental systems. Summarization of related techniques are shown in Table 2.1. The results and erosional factors from these techniques will be stated in the following section.

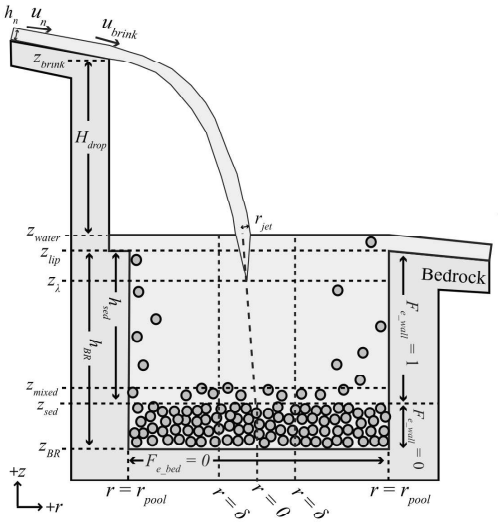

Figure 2.1 Schematic of plunge pool (Scheingross & Lamb, 2017).

Table 2.1 Summarization techniques for accessing the erosion process.

Approach	Technique	Advantage and Limitation	References
Field testing	Erosion rate measurement	• Variation devices for short- and long-term measurements. • The cost for instruments are expensive.	Inkpen and Jackson (2000); Trudgill et al. (1989); Lyles (1983)
	Topography observation	• Highly discontinuous in time are shown along fracture pattern in field. • Persistence of slopes are expressed with a short time scale (typically 0.1-10 Ma).	Krautblatter and Moore (2014)
	Trajectory and distances measurement	• Size effect, properties of rocks, and transportation surface can limit the mobility of rock.	Shrestha (2008); McCarroll and Nesje (1996)
Laboratory testing	Weight loss measurement	• Provide a relative rate. Degradation rate can be calculated with density of rock.	Gapta and Seshagiri (2000); Ergular and Shakoor (2009); Torabi-Kaveh et al. (2021); Torsangtham et al. (2019)
	Surface observation	• Provide a relative value to study the degradation behavior.	Fuenkajorn (2011); Kolay and Kayabali (2006)
	Relative rate measurement from input and output force	• The relative force simulating with field data are concerned • Various of techniques (i.e., Plunge pool, water jet and aerial jet).	George and Sitar (2012); Scheingross and Lamb (2017); Xiang, Latham, and Pain (2022)
Numerical simulations		• Limitation of input and physical parameters of rocks • The effect of scrubbing and colliding of rock need to be concerned	Inkpen (2007)

The mechanisms such as mechanical and chemical erosion are exhibited similarly with weathering. The degradation assessment for erosion process then can be expressed in terms of durability of rocks.

As recommended by the American Society for Testing and Materials Standard, ASTM-D4644 (2016), slake durability index test is one of the techniques for rock durability assessment which indicates the capacity of rock degradation in laboratory conditions.

The mentioning test, originally proposed by Franklin and Chandra (1972) for evaluating the durability and potential to degradation of rock. Their approach utilizes two cycles for wetting and drying of slake tests as the assessment method to observe the degradation capacities by tracking mass loss after each test cycle, the following relationship defines the durability at test cycle i:

$$Id_i = (m_i/m_0)\times 100 \tag{2.1}$$

where Id_i is the durability index at test cycle i (%), m_i is the mass of a retained samples after test cycle i (g), m_0 is the mass of initial samples (g), and i represent the number of test cycles.

Ergular and Shakoor (2009) analyze statistical relationships between the degradation rate of clay-bearing rocks and grain distribution sizes with the increasing of durability test cycles. Grain size distribution curves are projected to correlate with the concept of disintegration (degradation) ratio, D_R as follows:

$$D_R = A_C/A_T \tag{2.2}$$

where A_C is the ratio of area under particle size distribution curves (m^2) and A_T is the total area encompassing all particle size distribution curves (m^2).

Zhu and Deng (2019) propose a classification for red beds, clay-bearing rocks from central Yunnan, China. Their classification scheme utilizes both particle size distribution and durability index. The durability index is expressed as:

$$Id_i = (m_i/m_{i-1}) \times 100 \quad (2.3)$$

where m_{i-1} is the mass of oven-dry sample before cycle i. The equation defines relative index based on Franklin and Chandra (1972) but emphasize its effectiveness reflecting the disintegrating capacity on each test cycle.

2.3 Erosional factors

To understand factors governing degradation processes, the approach to assess these alignment factors are reviewed in Section 2.2. In erosional term, not only the externals that are concerned but for internal factors, many researchers try to reach the physical properties of rocks to explain its behaviors. The specific factors controlling such process are alternatively expressed by various researches to reflect the environment matching with their concertation. The relative importance of these factors are varied between field scale and laboratory setting. For laboratory, the specific conditions are controllable to identify the dominant of internal factors, compared to the complex conditions in the environments.

2.3.1. Fluvial factors

Within the context of fluvial systems, Luc, Lomine, Poullain, Sail, and Marot (2015) and Flores, Cuhaciyan, and Wohl (2006) identify dominant factors influencing erosion process include external dynamic energy, scale-dependent relationships, and hydroclimatic controls. Their findings are summarized as follows:

1) External energy

The dynamic energy from water flow, i.e., stream power, influenced by factors such as bedforms and fluid volume in the system. Particle or fragment that reaches high magnitude of energy from a flume bed might exhibit different degradation from those low energy in flat areas.

2) Scale-dependent

Sizes of the streamline are varied depending on patterns of the system. The factor is influenced the reaching distance of particle (fragment) displacing from the initial point. The streamline scale governing particle transport in varies magnitudes.

3) Hydraulic and hydroclimatic parameters

The climatic factors are related to fluid flow through rock matrix, i.e., corrosion, include with the hydraulic shear stress, cohesion between grains, pore fluid pressure, hydraulic gradient and related factors, e.g., rainfall, evaporation, and runoff dynamics within a watershed.

2.3.2. Aeolian factors

Zobeck et al. (2003) analyze the complex of external features governing wind erosion in aeolian environments. The factors involve with the climatic conditions, particle characteristics, and bedform features. Their findings emphasize the importance to consider these factors when assessing wind erosion at the field scale. To clarify this concept, Shrestha (2008) represents a functional relationships to express degradation rates (D) as:

$$D = f(I,K,C,L,V) \tag{2.4}$$

1) Fragment erodibility, I

Erodibility factor represents the susceptibility to erosion, involves with grain sizes, texture, mineral composition and topography feature.

2) Surface roughness, K

Roughness factor accounts for surface irregularities. This factor reducing the erosion by disrupting the impact of wind flow. A rougher surface generally leads to a lower process, representing as a protection against wind erosion. While fragments with higher erodibility tend to lose their surface roughness faster.

3) Climatic erosivity, C

This factor is significant impacted the climatic processes from windspeeds and surface moisture. The calculation for the C factor is represented as $C = 386 \cdot u^3 / (PE^2)$, where u denotes average wind velocity and PE signifies the precipitation index.

4) Unsheltered distance, L

Unsheltered distance represents the distance across a field where erosive winds can freely transport, which directly influenced amount of particles carried by wind power.

5) Vegetation cover, V

The equivalent vegetation cover are accounted for the protective against wind erosion. This factor is determined by comparing the existing vegetation to a reference condition called “Small Grain Equivalent, SGe”. The effectiveness of vegetation for reducing erosion depends on its characteristics.

2.3.3. Laboratory factors

In additional to above considerations, Moses et al. (2014) express that the factors impacting erosion correspond to surface roughness and texture, depth and extent of weathering in matrix, mineral alteration, and rate of material loss from the surface. These results have been confirmed with Gapta and Seshagiri (2000), Lashkaripour and Boomeri (2002), Ergular and Shakoor (2009), Torabi-Kaveh, Mehrnahad, Morshedi, & Jamshidi (2021), and Jamshidi (2023) studies. The degradation rates are varied for different rock types, according to their physical, chemical, and mechanical properties. These factors are summarized as follows:

1) Surface roughness

The erodibility of outer surface, while rocks moving through the systems, e.g., wind and water are increased chance of rock surfaces to interact with environment conditions. The difference of degradation creates surface roughness on a specific rock types.

From findings of McCarroll and Nesje (1996), the variation of degradation rates are influenced from mineral composition and leading to a rough surfaces. The scale of roughness are varied with sizes of mineral grain in the matrix of rock. From their study, three boulders with varying of mineral grain sizes (e.g., 4 cm , 2 cm, and 1 cm) are measured near the cliff and in the splash zone. The results show a significantly altered surface to roughness with a maximum scale of grain sizes, where the transport of boulder fragment (large grain sizes within the matrix) from the cliff to splash zone, tend to have a coarser surface within the process. In Figure 2.2, the fragments are smoothed by marine erosion (below high water). The roughness surface value are maximized mostly near the cliff as shown within a drastically profiles. This agrees with the results obtained by Inkpen (2007), who explained that the impact of erosion on rock surface are depended on the relationship between erosion rates and the height of slope. His results show that the different points of height tend to give more durable

to fragments, comparing to a higher degrade of rock surface under flat area. The transport duration of fragment is insignificantly effected the degradation rate. Figure 2.3 shows the simulation of a fragment transport in a different of slope height.

Fuenkajorn (2011) simulates the degradation process of weak rocks including volcanic, metamorphic, and sedimentary rocks with repeated test cycles on the durability test. The results reveal two different patterns based on rock fragment textures (Figure 2.4). Rocks with uniform texture throughout (inner matrix to outer surface) exhibited a relative decrease in durability with test cycles. The uniform texture is suggested on a consistency level of weathering and hardness across the fragment, where a lower durability fragment is degraded faster. Rocks with non-uniform texture tend to have a weaker surface than the inner matrix and results dramatically increased in degradation rate. The transition of rock matrix durability is varied, depending on rock type and weathering degree.

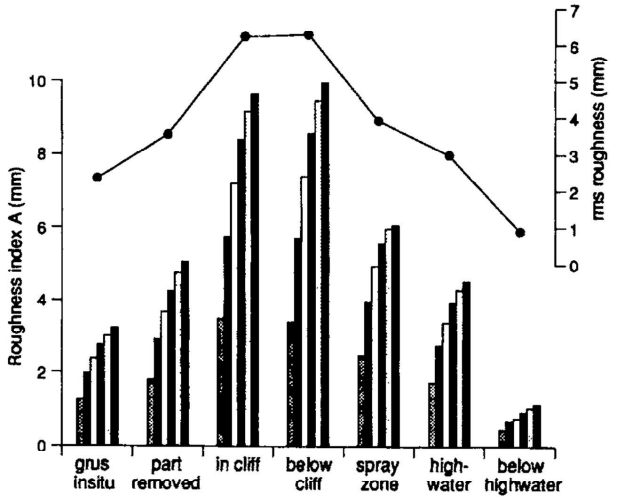

Figure 2.2 Surface roughness profiles in variation systems, the bars represent intervals of 5, 10, 15, 20, 25 and 30 mm, from left to right (McCarroll & Nesje, 1996).

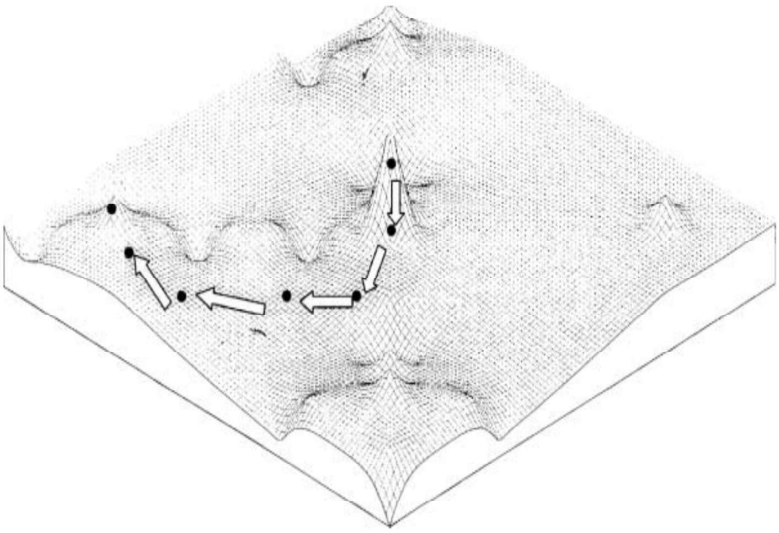

Figure 2.3 Simulation of fragment transport in different points of slope height (Inkpen, 2007).

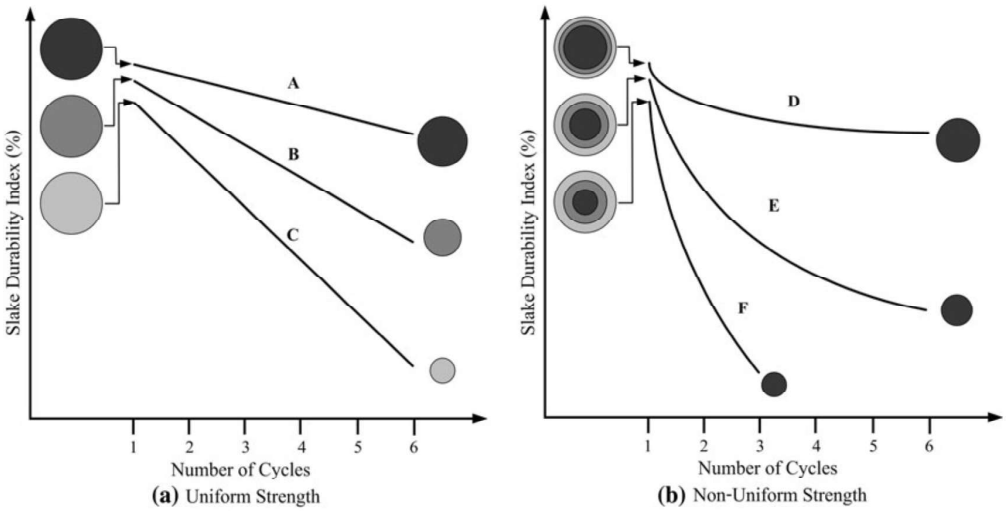

Figure 2.4 Rock degradation concept. Samples A, B and C (a) represent uniform texture. Samples D, E and F (b) represent weathered zone outside and fresher matrix inside (Fuenkajorn, 2011).

2) Mineral alteration

Gokceoglu, Ulusay and Sonmez (2000) correlate relationships of mineral characteristics in weak rocks. They mentioned that clays content, especially smectite, controls the variation of durability. Higher percentage of clays in claystone and ignimbrites causes a significant low durability in the second through fourth cycles from 0 to 70%, where values of durability agree to high carbonate content (Figure 2.5). They also introduce the estimation of quantitative minerals for particles passing from the drum after each slake durability test cycle. The removing rate of these minerals depend on the number of cycles. The cumulative quantities of each mineral (Q_m) is determined as:

$$Q_m = \sum_{i=1}^{i} \{[(Id_i - Id_{(i+1)})(Y_{X_i} / 100)] / Y_{X_0}\} \quad (2.5)$$

where Id_i is the durability index at test cycle i (%), Y_{X_i} is the percentage of each mineral from passing material at test cycle i (%), determined by X-ray diffraction (XRD) analysis, Y_{X_0} is the number of minerals and i is the number of cycles.

They also analyze passing materials with grain size distribution using wet sieve and hydrometer techniques. Their results reveal a significant decrease in fragment sizes correspond to passing materials with increasing test cycles (Figure 2.6). They define that the dominant particle size falls within the silt range, according to the mechanisms of scrubbing and crushing experienced during the tests.

Hawkins and McConnell (1992) investigate physical properties of British Isles argillaceous rocks and find that sandstone is mostly susceptible to water due to clay expansive forces and ferruginous cementing within their matrix. They also determine the quartz-clay framework through the effects of clay content, cementation, and mineral compositions on the durability of sandstones. The results indicated that clay contents contribute to a highly degraded when encounter with water. Ferruginous

and calcareous cementations are generally more susceptible than those with siliceous cement under submerging stage. However, they noted that chlorite might play a critical role in strength loss than swelling clay minerals, due to its complicated structure.

The result obtained from Hawkins and McConnell aligns with those of Lin, Jeng, Tsai, and Huang (2005), who study sandstones with significant clay contents. They state that chlorite might be the primary factor influencing the susceptibility of sandstones to degradation during submersion. They give an explanation that it probably due to the leaching potential, which appears to impact than the swelling behavior of clays. According to Figure 2.7, chlorite is significantly loss after subjecting to water, compared to clays contents.

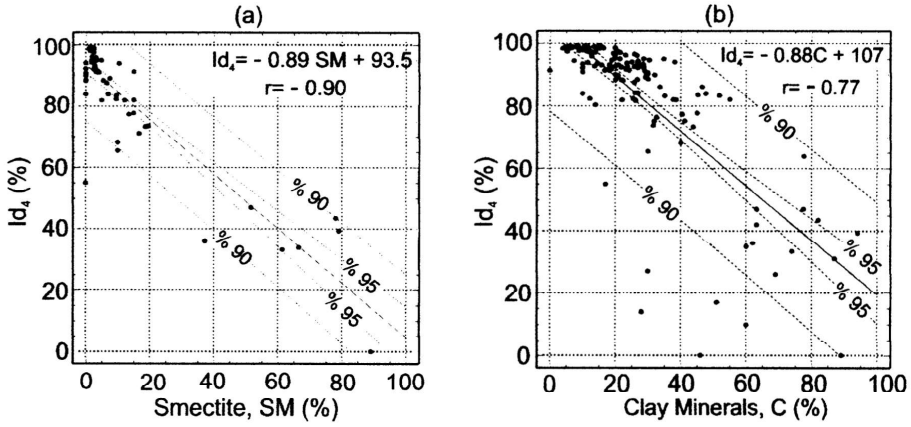

Figure 2.5 Regression of durability with expansive clay (a), and total amount of clay minerals (b) for all rock types (Gokceoglu, Ulusay, & Sonmez, 2000).

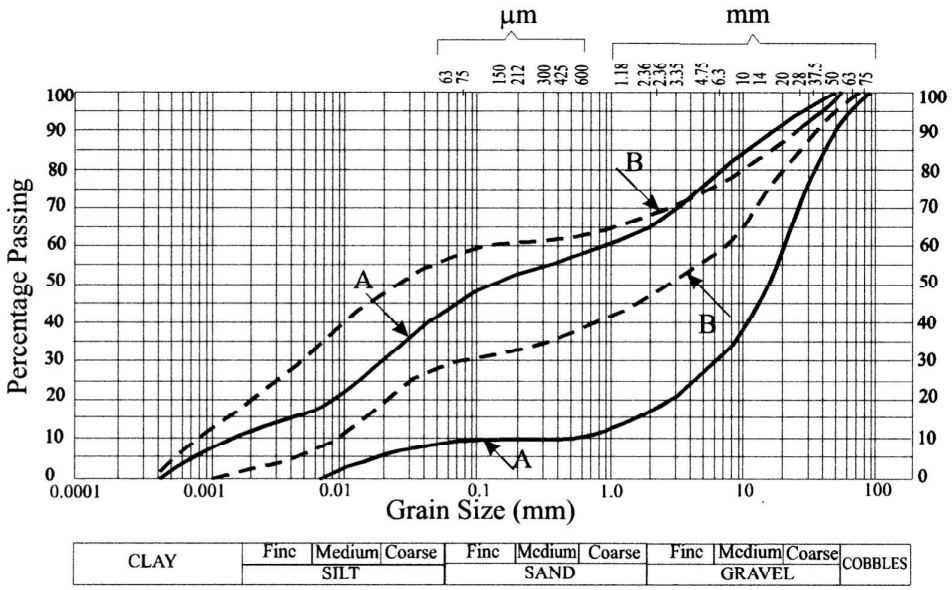

Figure 2.6 Percentage of passing material with a function of grain sizes (Gokceoglu, Ulusay, & Sonmez, 2000).

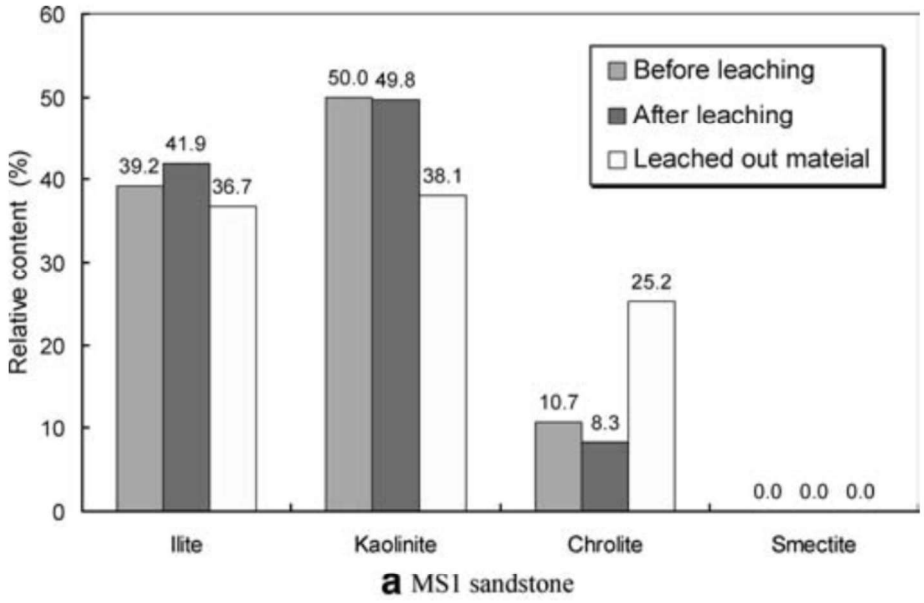

Figure 2.7 Relative clay contents and chlorite in sandstones with variation of stages (Lin et al., 2005).

3) Texture and packing density

Heidari, Momeni, Rafiei, Khodabakhsn, and Torabi-Kavah (2013) state that the effects of rock textures (e.g. fine-grained matrix, grain network, and cementing agent), affect degradation process more than mineral compositions and conclude that rock textures are more noticeable in a relationship for predicted engineering characteristics.

To reveals a significant connection between packing density, grain contact, and porosity, Dobereiner and Freitas (1986) define that grains of sandstones with lower degrees of tangential grain contacts are exhibited floting within the matrix of rock fragment. As packing density increases, the percentage of contacting grains are raised between 25% to 30% causing the strengthen in cementation and internal components inside the matrix. This agrees with Lin et al. (2005), their result shows non-effective of packing density in sandstones with the tangential grain contacts above 60%.

Koncakul and Santi (1999) express a relationship between packing density, porosity, and permeability. They state that the decrease of porosity and permeability are due to packing density that limit the water pass through the matrix and maximizing its durability. The results tend to agree with Corominas, Martinez-Bofill, and Soler (2014) and Sousa, Surarez del Rio, and Calleja (2005), who study the influence of physical properties and microfractures. They conclude that porosity is one of the primary factors that controls the intensity of physical and chemical alterations within rock.

Additional to these factors, the textural feature of rock fragments including their shape and size also affect the erodibility of rock, as evidenced from the results obtained by Gong, Zhu, and Shao (2018), Lamb, Finnegan, Scheingross, and Sklar (2015), and Li, Fu, Hu, and Liu (2022). These studies indicate that the differences

of fragment shapes tend to give the alternative results for durability assessment of erosion.

From the study of Kolay and Kayabali (2006), they use the concept of factual dimension to calculate the effect of shapes use in the durability test and conclude that spherical shape exposes less surface area, compared to cubic and triagonal prism shapes. Their results also show that rougher surface further develops a higher angularity. As fragment become less in spherical, the higher of surface area leading change for rock fragment to expose through water and accelerated the degradation process. The relationships between variation shapes are expressed below:

$V_{sphere} = V_{cube} = V_{tr.\ prism}$

$4.19r^2 = b^3 = 0.43a^2$

giving $r^2 = 0.38b^2$, $a^2 = 1.75b^2$

if $A_{sphere} = 4\pi r^2$, $A_{cube} = 6b^2$, and $A_{tr.\ Prism} = 3.87a^2$

$A_{sphere} = 4\pi(0.38b^2)$, $A_{cube} = 6b^2$, and $A_{tr.\ prism} = 3.87(1.75b^2)$

$A_{sphere} = 4.83b^2 < A_{cube} = 6b^2 < A_{tr.\ prism} = 6.78b^2$

where a and b is dimentional axis of cubic and triangonal prism shapes, r is radius of sphere shape (mm), A is surface area of fragment (mm^2), and V is volume of fragment (mm^3). Figure 2.8 shows evaluation parameters within the different geometrical shapes.

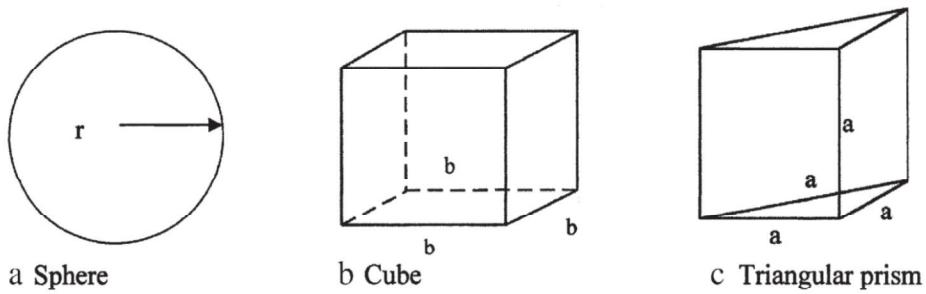

Figure 2.8 Geometrical shape parameters of spherical (a), cubic (b) and triangular prism (c), (Kolay & Kayabali, 2006).

4) Pore pressure

The impact of water intrusion on internal structure is weakened the cohesive forces between mineral grains and giving change of water to interact between grains contact, resulting in a reduce of intergranular frictional resistance (Koncagul & Santi, 1999).

According to Lin et al. (2005), who study the micromechanisms of sandstones influenced by the water pressure. They reveal that the presence of water varies the fracture behaviors of sandstones. Sandstones under dry condition tend to propagate cracks within mineral grains (intracrystalline), while saturated sandstones, particularly with low chlorite content, exhibit cracks between grains (intercrystalline). Figure 2.9 shows a variation of fractures occur within sandstones.

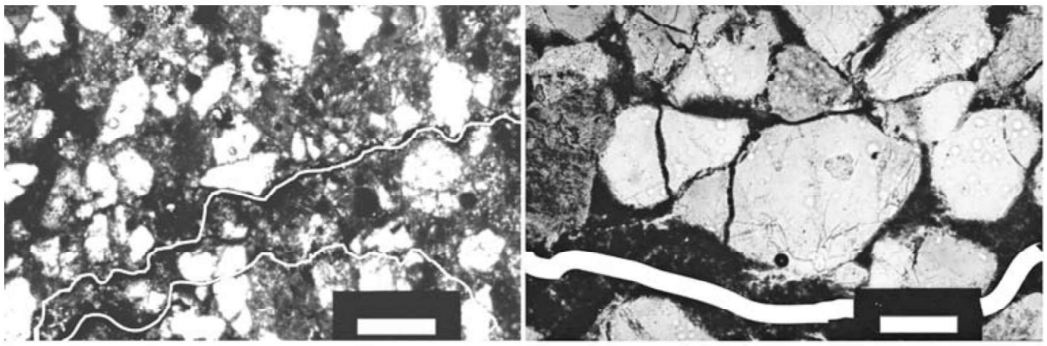

Figure 2.9 Petrographic images of intergranular fracture (a), and intragranular fracture (b) in sandstone (Lin et al., 2005).

5) Internal stresses

The stresses within rock matrix arise from a complex relationship between the factors and correspond to input mechanism in the systems. Current researches have analytically explored the nature of force-induced stresses experienced within rock matrix and upon their surfaces. The inducing forces are considered with many perspectives, including terms of temperature and hydraulic stress.

Thermal expansion induced by the variation change of temperatures to the composing minerals within rocks. Sandstones that contain mostly quartz and feldspar whose thermal expansion coefficients are similar with a high range of heat capacity are more durable (Somerton, 1992). From the study of Li and Liu (2022), Sandstone masses are slightly decreased when temperature is less than 400 °C. They state that high temperature has a significant deteriorating effect, where cracks due to thermal damage show when temperature reaches over 400 °C.

For rocks containing minerals with different thermal properties, such as igneous rocks, the effect of temperature becomes significant. McKay, Molaro, and Marinova (2009) study the degradation behavior influencing by temperature changing on surface of igneous rocks, specified on dry (wind) areas. The thermocouples are used as a site equipment and measure with a constant time intervals (dT/dt). The results obtained from their study shows the similarity distribution of dT/dt values in all conditions. They indicate that thermal stresses from variation of temperatures are significantly cause microcracks and fractures within rock matrix. They also state that the thermal stress might be a significant contributor to the physical spalling and flaking on rock surface.

Tugrul and Zarif (1998), Gokceoglu et al. (2000) and Torabi-Kaveh et al. (2021) give the explanation on the hydraulic stress. Sandstones with clay minerals are directly reduced their durability due to the release of residual stresses within the rock

matrix. This release of stress destabilizes the internal structure and accelerates its degradation during submersion.

6) Duration and replete cycles

The duration of testing is significance for assessing durability. Lin et al. (2005) explain the assessments with extended periods, revealing that the degradation rates are increased with prolonged submersion, which directly cause more interaction time between water and internal structure of rocks. They also state that the densities are decreased around 0.5 g/CC after a period of submersion. As the porosity increases, the mineral contents within the matrix appear to become less cohesive and easily to reach out with water (Figure 2.10). This finding agrees with the results of Zhou, Cai, Ma, Chen, Wang, and Tan (2018), they observe water ingression into the matrix of sandstones, within 24 hours the percentage of water is linearly increased up to 3% (Figure 2.11). Their results show that after repeating of cycles, the durability and density tend to decrease with an increasing of porosity, where it corresponds with the submerging time (Figure 2.12).

Gokceoglu et al. (2000) investigate the influence of test cycles on durability for various rock types from Turkey. The statistical analyses from their results are utilized as the influence of cycles on the degradation rate. The results show that the coefficient between these relationships is relatively increased with test cycles, causing the intergranular bond to become weakening and developed the microcracks within rock matrix.

This agree with the results obtained by Fereidooni and Khajevand (2017) and Torsangtham, Khamrat, Thongprapha, and Fuenkajorn (2019), who investigate rock durability through 100 cycles of a slake durability tests under wet, dry, and acidic conditions on carbonates, granites, sandstones, and basalts. The results show that in long-term, granite durability deteriorates under exposure through water and acidic

conditions, due to their structures such as pore matrix and ferrous oxide cementation, which leading to microcracks. The study also reveals that sandstones degrade highest under wet conditions due to expansive clays in their matrix.

Walsri, Sriapai, Phueakphum, and Fuenkajorn (2012) simulate sandstones degradation using a large-scale slake durability test device and perform 100 cycles under dry and wet conditions. Test results show the sensitivity of sandstones are severed as submerged in a prolong cycles. The degradation rate after submerging to water is increased than under dry condition.

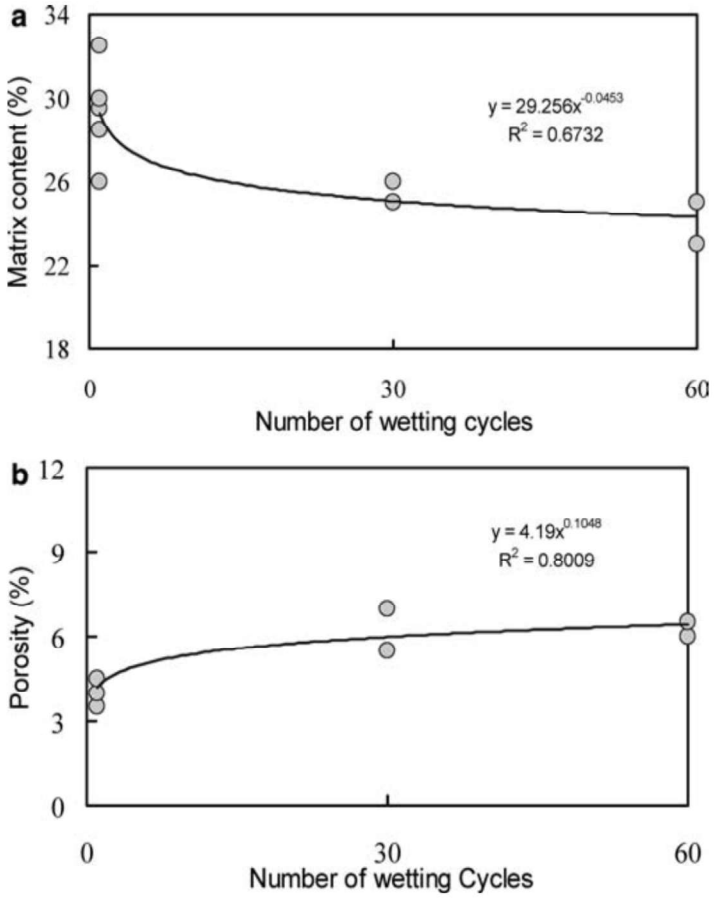

Figure 2.10 Influence of cycles to matrix content and porosity of sandstones (Lin et al., 2005).

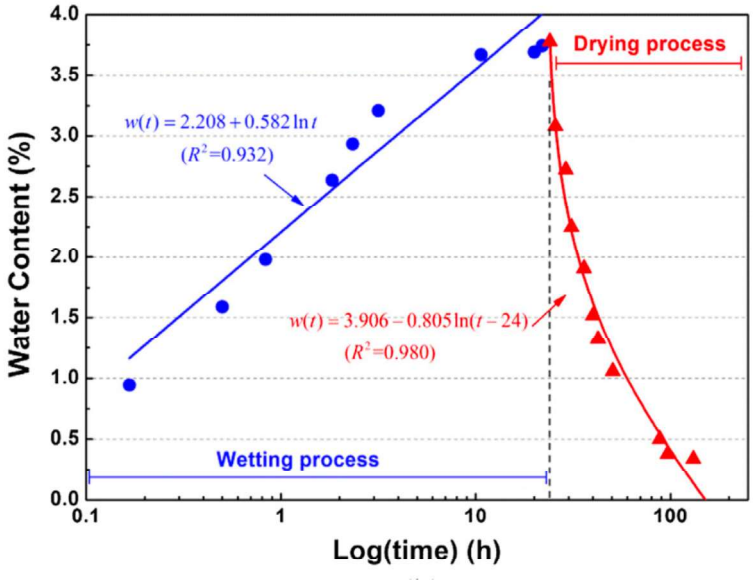

Figure 2.11 Water content in a function of time duration (Zhou et al., 2018).

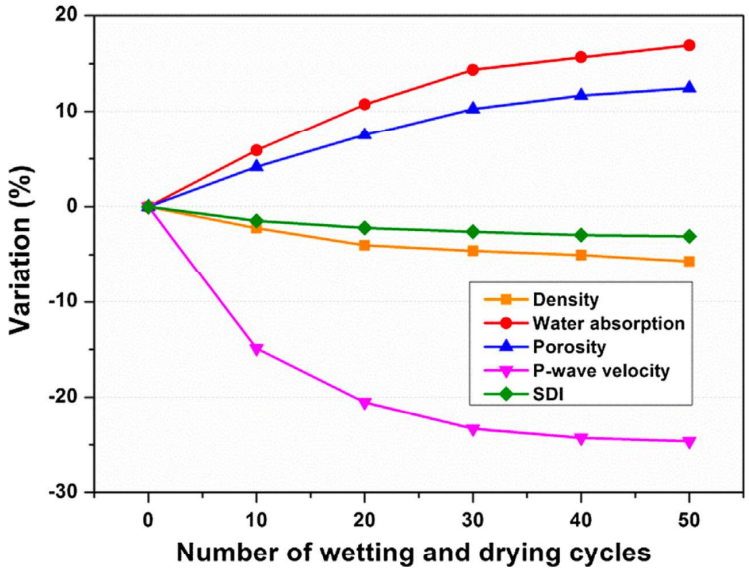

Figure 2.12 Percentage of variation properties with a number of wetting and drying cycles (Zhou et al., 2018).

2.4 Erosive energy

Mathematical evaluation of energy requisites for rock degradation is developed with multi-perspectives. The current approaches to resolve energies are incorporated in a wide range of concepts across many disciplines, considered reflective to environment conditions. Recent researches attempt to define the connection between energy and degradation mechanisms with field monitoring data, visual observation, and simulation techniques (detailed in section 2.2). To clarify the perspective, the reviews are focused on the classification of processes, while the origin of forces are addressed in a subsequent section.

2.4.1 Wind process

Aeolian degradation process, or wind erosion is influenced by a complex factors (detailed in 2.3). The sufficient volume of windspeeds can transport the fragment or particle through saltation, creep, or suspension. Lyles (1983) defines the erosive wind energy using extensive field data from aeolian area in North America. She uses the erosive potential from windspeeds profile to estimate the annual erosion rate. The following equation is determined the relationship of energies as:

$$E_p = (EWE) \cdot (E_a) \tag{2.6}$$

where E_p represents estimated erosion over a defined period (mm/yr), EWE is proportionality constant reflecting erosive wind energy at a specific location (J), and E_a is the estimated annal erosion (mm/yr). She state that terrain and temperature need to be concerned, where the temperature below subzero causes particles in solid state.

Shrestha (2008) develops an equation to estimate erosive wind energy (EWE) with an hourly windspeeds data. The equation is expressed as:

$$EWE = 3600 \cdot \rho \cdot (U^3 - U_T^2) \tag{2.7}$$

where *EWE* is the hourly erosive wind energy (J), ρ is the wind density (g/m), U and U_T are the average hourly windspeeds and average hourly threshold windspeeds (m/s), respectively.

2.4.2 Stream (Water) process

Larimer, Yager, Yanites, and Witsil (2020) investigate the energy transfers by mechanical impacts during particles and observe the saltation behavior on planar and non-planar bed surfaces. They propose the equations defining rates of kinetic impact energy, which involving with the magtitude impact of the energy and rate of impaction. The relative eqution are state as follows:

$$\varepsilon_{kr}^{*} = \frac{q_s [\sin(\vartheta - \varphi) \cdot V_{si}]}{2 \cdot R_b g \, l_s} \tag{2.8}$$

where R_b is the buoyant density of particle (g/cc), g is gravity, h_s is the hop height (m), v_{si} is the vertical settling velocity (m/s), l_s is the horizontal displacement (m), ϑ is the angle relative to average bed slope (degrees), and φ is the surface angle of bedding (degrees). They state that the proposing equation is maximized the influence of non-dimensional transport. The relative factors include hydrodynamic forces, particle weight, relative fluid motion, particle rotation, and collisions with the bed and other grains. To address this complexity in relationship, the following are expressed in terms of transport trajectory (Wiberg & Smith, 1985):

$$T^{*} = \frac{\rho_w g R_h S}{(\rho_s - \rho_w) g D_s \cdot \tau_c^{*}} - 1 \quad , \tag{2.9}$$

where τ_c^{*} is the critical stress, ρ_W is water density, ρ_S is particle density, R_h is hydraulic radius, S is channel slope. From Wiberg and Smith, there are three factors related between saltation mechanisms (Figure 2.13):

the hop displacement:

$$l_s^* = \frac{l_s}{D_s} \ , \tag{2.10}$$

the hop height:

$$h_s^* = \frac{h_s}{D_s} \ , \tag{2.11}$$

and vertical-independent velocity:

$$v_{si}^* = \frac{\sin(\vartheta - \varphi) \cdot V_{si}}{\sqrt{(R_b\, g\, D_s)}} \tag{2.12}$$

According to the relationship of aforementioned equations. Wiberg and Smith state that the stress is significantly influenced the energy dynamics. The duration of particle transports directly corresponded with the rate of particle velocities. The displacement of particle hopping decreases the dynamic of kinetic energy to bed load. They note the effect on flow direction, considered on the turbulence flow through the trajectory. The machanism of saltation with high inertia in the matrix seem to diminish the fluctuations. However, for interpretating on the kinetic energy impact, the fluctuation effect still needs to be concerned.

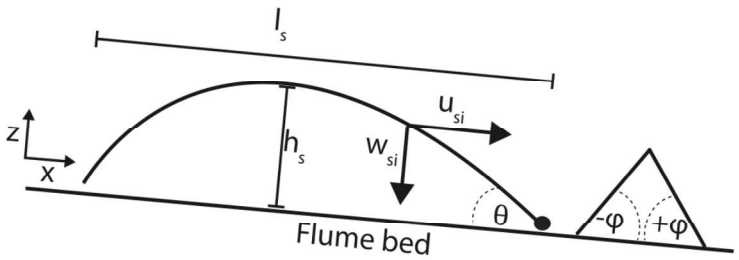

Figure 2.13 Saltation trajectory diagram (Larimer et al., 2020).

Marot, Le, Garnier, Thorel and Audrain (2012) propose a streamline approach to study the process and symplify the equation based on concept of fluid energy on fragment (particle) with diameter between 0.5 µm to 0.125 mm. They state that the relationship emphasizing on mechanical aspect as given parameters, including temperature and internal energy (intrafluid and pressure) in steady-state condition. The total energy dissipated from water flow are determined by integration of the erosion power (P) over the test duration as follows:

$$\frac{dE}{dt} = \frac{d}{dt}\int P = \frac{dW}{dt} = (\rho \cdot g \cdot \Delta z \cdot K) + (K \cdot \Delta P) \qquad (2.13)$$

where E is the total energy (J), W is work in process, ρ is density of fragment (g/cc), g is gravity, Δz is the distance of fragment transfers in the system (mm), K is fluid flow rate, and ΔP represent the power done in time duration. According to their analysis, the total energy varies from 40 to 490 J. They suggest that total energy under 60 J for fragments with diameter less than 0.125 mm (clay size) has no significant erosion that should be measured. They also correlate eroded mass with total energy dissipation (Figure 2.14). The results show that the quantity of eroded mass (g) exhibits a linear correlation with energy dissipation and can be expressed as $m_{erode} = 0.0017(E - 60)$.

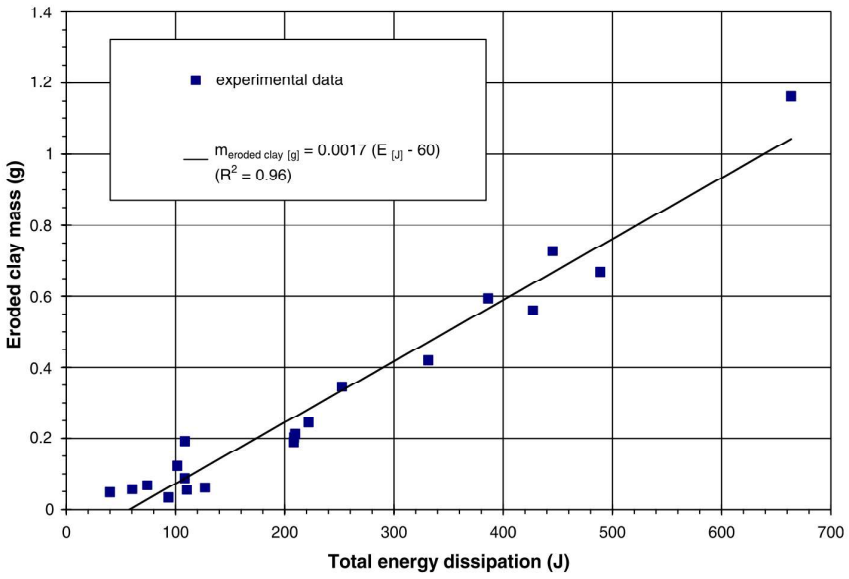

Figure 2.14 Eroded mass in a fuction of total energy dissipation (Marot et al., 2012).

Luc et al. (2015) analyze the internal erosion of rock fragments under water seepage and while fragments transport in the systems. They observe fragment behavior by deviding the processes as internal shear stress and flow power energies. The shear stress can be defined as:

$$\frac{d\varepsilon}{dt} = k_d \cdot (T_s - T_c), \qquad \text{if } T_s > T_c \tag{2.14}$$

where ε is rate of erode mass per unit of erosion surface area, k_d and T_c are parameters characterizing the sensitivity of the soil erosion, and T_s is hydraulic shear stress

Fuenkajorn (2011) proposes an energy absorption concept and correlates the simulation of durability test cycles with field data. The following equation is developed to evaluate heat energy absorbed by rock specimens as:

$$Q = \sum_{i=1}^{n} (m \cdot C_p \cdot \Delta T_i \cdot \Delta t_i) \tag{2.15}$$

where Q is absorbed energy of specimen (kJ), m is mass of specimen (kg), C_p is specific heat capacity (kJ/kg·K), ΔT_i is temperature change in Kelvin degrees, Δt_i is the time interval of energy absorption (hours) and n is the number of hours. The energy absorbed during heat simulation for a common rock is estimated as 4.320 MJ/h (where m = 5 kg, C_p = 0.90 kJ/kg K, ΔT_i = 80 K, and t = 12 h) and the coefficient of heat capacity varies between 0.6 and 1.2 kJ/kg·K. The limitation on variation change of temperature during simulations might induce damage to rock matrix compared to the gradual changes observing in field.